Supporting Information:

Fused Selenophene-thieno[3,2-*b*]thiophene-selenophene (ST)-based Low Bandgap Electron Acceptor for Efficient Organic Solar Cells with Small Voltage Loss

Xunfan Liao*[a†], Xueliang Shi[b†], Ming Zhang[e], Ke Gao[c], Lijian Zuo[c], Feng Liu*[e], Yiwang Chen*[a], Alex K-Y. Jen*[c,d]

[a]State Key Laboratory for Modification of Chemical Fibers and Polymer Materials & College of Materials Science and Engineering Donghua University, Shanghai 201620, China

[b]Shanghai Key Laboratory of Green Chemistry and Chemical Processes, School of Chemistry and Molecular Engineering, East China Normal University, Shanghai 200062, PR China

[c]Department of Materials Science and Engineering, University of Washington, Seattle, WA, 98195-2120, USA

[d]Department of Chemistry, City University of Hong Kong, Kowloon, Hong Kong

[e]School of Chemistry and Chemical Engineering, Shanghai Jiaotong University, Shanghai 200240, China

Corresponding author. Tel.: +86 791 83968703; fax: +86 791 83969561. E-mail:

xfliao616@dhu.edu.cn (X. Liao),

fengliu82@sjtu.edu.cn (F. Liu),

ywchen@ncu.edu.cn (Y. Chen),

ajen@u.washington.edu (A. Jen),

†These authors contributed equally to this work.

1. EXPERIMENTAL SECTION

1.1. Chemicals and Instrumentations. All reagents were purchased from commercial sources and used without further purification. Anhydrous dichloromethane (DCM) and N,N-dimethylformamide (DMF) were distilled from CaH_2. Anhydrous toluene and THF were distilled from sodium benzophenone immediately prior to use. The ^{1}H NMR and ^{13}C NMR spectra were recorded in solution of $CDCl_3$ on Bruker DRX 300 NMR spectrometer with tetramethylsilane (TMS) as the internal standard. High resolution (HR) electrospray ionization (ESI) mass spectra were recorded on LTQ Orbitrap XL™ Hybrid Ion Trap-Orbitrap Mass Spectrometer. UV-vis-NIR absorption spectra were recorded on a Varian Cary 5000. The electrochemical measurements were carried out in anhydrous DCM with 0.1 M tetrabutylammonium hexafluorophosphate ($Bu4NPF_6$) as the supporting electrolyte at room temperature under the protection of nitrogen. A gold disk was used as working electrode,

platinum wire was used as counting electrode, and Ag/AgCl (3M KCl solution) was used as reference electrode. The potential was calibrated against the ferrocene/ferrocenium couple.

1.2. Synthesis.

Synthesis of compound 3: Diethyl 2,5-dichlorothieno[3,2-b]thiophene-3,6-dicarboxylate 1 (706 mg, 2.0 mmol), and tributyl(2-selenophenyl)stannane 2 (2.52 g, 6.0 mmol) were dissolved in toluene (30 mL). $Pd(PPh_3)_4$ (100 mg) was added as a catalyst and the mixture was refluxed for 12 h under argon. After cooling down the solvent was evaporated to dryness under vacuum. The mixture was purified by column chromatography (silica gel, DCM) and product 3 was further purified by recrystallization from $MeOH/CH_2Cl_2$ as a yellow solid (1.0 g, 92% yield). ^1H NMR (300 MHz, $CDCl_3$, ppm): δ = 8.22 (dd, J = 5.7 Hz and 0.9 Hz, 2H), 7.77 (d, J = 3.8 Hz and 1.0 Hz, 2H), 7.37-7.33 (m, 2H), 4.42 (q, J = 7.1 Hz, 4H), 1.43 (t, J = 7.1 Hz, 6H); ^{13}C NMR (75 MHz, $CDCl_3$, ppm): δ = 162.02, 149.29, 138.37, 136.61, 135.36, 131.95, 129.38, 118.55, 61.39, 14.28; HR MS (ESI): calcd for $C_{20}H_{17}O_4S_2Se_2$ [(M+H)+], 544.8899; found, 544.8893 (error: -1.10 ppm).

Synthesis of compound ST: A flame dried flask equipped with a stir bar was charged with Mg turnings (0.144 g, 6 mmol), anhydrous THF (30 mL) and 4-hexyl-1-bromobenzene (1.45 g, 6.0 mmmol). The above mixture was heated to reflux until the Mg turnings totally disappeared. After cooling to room temperature, compound 3 (542 mg, 1.0 mmol) was added as solid in one portion. After this addition, the mixture was slowly heated to reflux for overnight. The reaction was quenched with 10% HCl solution (10 ml) and extracted twice with ethyl acetate. The organic layer was dried (Na_2SO_4), filtered, and evaporated to dryness under vacuum. After that the crude diol was dissolved in anhydrous toluene (80 mL) and the whole system was degassed via three freeze-thaw pump cycles. To the mixture, an excess of amberlyst 14 (about 0.3 g) was added in onel portion under argon atmosphere. The mixture was heated to 80 °C for 5 hours. After that the reaction was filtered to remove amberlyst 14, and concentrated under vacuum. The residue was purified by column chromatography (silica gel, hexane: DCM 5:1 v/v). Compound ST was further purified by recrystallization from $MeOH/CH_2Cl_2$ as a yellow solid (766 mg, 72% yield for two steps). ^1H NMR (300 MHz, $CDCl_3$, ppm): δ = 7.79 (d, J = 5.4 Hz, 2H), 7.28 (d, J = 5.4 Hz, 2H), 7.13 (d, J = 8.2 Hz, 8H), 7.07 (d, J = 8.2 Hz, 8H), 2.55 (t, J = 7.8 Hz, 8H), 1.65-1.52 (m, 8H), 1.38-1.25 (m, 24H), 0.93-0.81 (m, 12H); ^{13}C NMR (75 MHz, $CDCl_3$, ppm): δ = 158.56, 147.96, 141.68, 139.82, 139.68, 139.00, 134.74, 129.98, 128.46, 127.79, 125.65, 63.03, 35.57, 31.68, 31.24, 29.13,

22.57, 14.07; HR MS (ESI): calcd for $C_{64}H_{73}S_2Se_2$ [(M+H)+], 1065.3484; found, 1065.3477 (error: -0.66 ppm).

Synthesis of compound ST-CHO: Compound ST (532 mg, 0.5 mmol) was dissolved in DMF (5 mL) and 1,2-dichloroethane (30 mL). An excess amount of phosphorus oxychloride (1 mL) was added and the mixture was stirred at 80 °C overnight. The reaction was quenched with saturated sodium acetate solution (10 ml) and stirred for 30 min at room temperature. The mixture was extracted twice with DCM, the organic layer was dried (Na_2SO_4), filtered, and concentrated under vacuum. The residue was purified by column chromatography (silica gel, hexane: DCM 1:2 v/v). Compound ST-CHO was further purified by recrystallization from $MeOH/CH_2Cl_2$ as a yellow solid (509 mg, 91% yield). ^1H NMR (300 MHz, $CDCl_3$, ppm): δ = 9.68 (s, 2H), 7.90 (s, 2H), 7.11 (s, 16H), 2.57 (t, J = 7.8 Hz, 8H), 1.65-1.51 (m, 8H), 1.42-1.22 (m, 24H), 0.93-0.82 (m, 12H); ^{13}C NMR (75 MHz, $CDCl_3$, ppm): δ =183.47, 159.56, 151.67, 149.77, 149.09, 142.53, 141.62, 138.18, 137.39, 134.53, 128.83, 127.54, 63.44, 35.54, 31.65, 31.21, 29.07, 22.54, 14.05; HR MS (ESI): calcd for $C_{66}H_{73}O_2S_2Se_2$ [(M+H)+], 1121.3382; found, 1121.3392 (error: 0.89 ppm).

Synthesis of compound STIC: Compound ST-CHO (168 mg, 0.15 mmol) and 3-(dicyanomethylidene)indan-1-one IC (117 mg, 0.6 mmol) were dissolved in 1,2-dichloroethane (12 mL) and EtOH (6 mL). A catalyst amount of beta-alanine was added and the mixture was stirred at 80 °C overnight. After cooling down, the reaction mixture was concentrated under vacuum. The residue was purified by column chromatography (silica gel, DCM). Compound STIC was further purified by recrystallization from $MeOH/CH_2Cl_2$ as a dark solid (200 mg, 91% yield). ^1H NMR (300 MHz, $CDCl_3$, ppm): δ = 8.93 (s, 2H), 8.68-8.62 (m, 2H), 7.92-7.84 (m, 4H), 7.76-7.67 (m, 4H), 7.14 (s, 16H), 2.58 (t, J = 7.8 Hz, 8H), 1.68-1.58 (m, 8H), 1.40-1.25 (m, 24H), 0.9-0.84 (m, 12H); ^{13}C NMR (75 MHz, $CDCl_3$, ppm): δ =189.06, 161.63, 161.24, 160.00, 153.95, 144.49, 143.05, 142.71, 141.74, 140.65, 139.91, 139.61, 137.73, 136.62, 134.91, 134.08, 128.99, 127.59, 125.09, 123.49, 120.34, 114.95, 68.01, 63.14, 35.57, 31.65, 31.21, 29.07, 22.55, 14.06; HR MS (ESI): calcd for $C_{90}H_{80}N_4O_2S_2Se_2$ (M+), 1472.4053; found, 1472.4059 (error: 0.41 ppm).

1.3. Theoretical Calculations. We performed quantum chemical calculations with the Gaussian 09 software package by selecting the 6-31G(d, p) basis set. The ground-state geometries were optimized by virtue of the popular B3LYP exchange-correlation functional.

1.4. Device Fabrication.

Organic solar cells (OSCs) were fabricated in the configuration of the traditional sandwich structure of ITO/PEDOT:PSS/active layer/C_{60}-bissalt/Ag. ITO-coated glass was cleaned by ultrasonic agitation in acetone, detergent, deionized water and isopropanol sequentially followed by plasma treatment for 3 min. Then the PEDOT:PSS (Baytron PVP 4083) was spin-cast on the ITO glass at 4000 rpm for 30 s and annealed at 150 °C for 10 min in air. The devices were transferred into a glovebox filled with N_2. Active layer solutions (PBDB-T:Acceptor weight ratio is 1:1.5) were prepared in CB (chlorobenzene) with or without 0.5% DIO. The total active layer solution concentration is 25 mg ml^{-1}. Then the active layers were spin coated from the PBDB-T:Acceptor solution on the substrates with 3000 rpm spin-coating speed to form about 100 nm film thickness. Finally, the C_{60}-bissalt dissolved in methanol with a concentration of 2 mg/ml was spin-coated on top of active layer. The device fabrication were finished by depositing 150 nm Ag in vacuum chamber of 10^{-7} Torr. Typical cells have devices area of 3.14 mm^2, which is defined by a metal mask with an aperture aligned with the device area.

1.5. Characterization of OSCs

The I-V characteristic curves were recorded in a Keithley 2400 source unit under a simulated solar irradiance (solar simulator from Newport Inc.) A certified silicon diode, which can be traced back to NREL, is used to calibrate the illumination intensity to 1 sun (100 mW/cm^2). A neutral filter is used to study the light intensity dependent device performance. EQE spectra were measured in a assembled setup including a stable light source, light chopper, monochromator, and lock-in amplifier.

1.6. SCLC measurements

The electron-only device with structure of ITO/ZnO/ PBDB-T:Acceptor/C_{60}-bissalt/Ag were fabricated. The carrier mobilities were measured using the space-charge-limited-current (SCLC) model, which is described by:

$$J = 9\varepsilon_0\varepsilon_r u V^2/8L^3$$

where J is the current density, L is the film thickness of active layer, ε_0 is the permittivity of free space (8.85×10^{-12} F m^{-1}), ε_r is the relative dielectric constant of the transport medium, u is the hole or electron mobility, V is the internal voltage in the device and $V = V_{appl}-V_r-V_{bi}$,

where V_{appl} is the applied voltage to the device, V_r is the voltage drop due to contact resistance and series resistance across the electrodes, and V_{bi} is the built-in voltage due to the relative work function difference of the two electrodes. The thickness of the BHJ blend for SCLC measurement was about 100 nm. The hole and electron mobility can be calculated from the slope of the $J^{1/2} \sim V$ curves.

1.7. Morphology Characterization

Grazing incidence x-ray diffraction (GIXD) characterization of active layer was performed at beamline 7.3.3, Advanced Light Source (ALS), Lawrence Berkeley National Lab (LBNL). X-ray energy was 10 keV and operated in top off mode. The scattering intensity was recorded on a 2D image plate (Pilatus 1M) with a pixel size of 172 m (981 × 1043 pixels). The samples were ~10 mm long in the direction of the beam path, and the detector was located at a distance of 300 mm from the sample center (distance calibrated by AgB reference). The incidence angle was chosen to be 0.16° (above critical angle) for GIXD measurement. OPV samples were prepared on PEDOT:PSS covered Si wafers in a similar manner to the OPV devices. RSoXS was performed at beamline 11.0.1.2 Lawrence Berkeley National Lab. Thin films was flowed and transferred onto Si_3N_4 substrate and experiment was done in transition mode.

2. SUPPORTING TABLES AND FIGURES

Table S1 Crystal data and structure refinement for STIC.

Empirical formula	C92 H82 Cl6 N4 O2 S2 Se2
Formula weight	1710.35
Temperature	100(2) K
Wavelength	0.71073 Å
Crystal system	Monoclinic
Space group	P 2_1/c
Unit cell dimensions	a = 17.568(7) Å $\quad\quad$ α = 90°.
	b = 21.991(11) Å $\quad\quad$ β = 104.87(2)°.
	c = 21.812(9) Å $\quad\quad$ γ = 90°.
Volume	8145(6) Å³
Z	4
Density (calculated)	1.395 Mg/m³
Absorption coefficient	1.208 mm⁻¹
F(000)	3520
Crystal size	0.150 x 0.070 x 0.002 mm³
Theta range for data collection	1.515 to 25.667°.
Index ranges	-20<=h<=20, -19<=k<=26, -26<=l<=26
Reflections collected	19414

Independent reflections	14797 [R(int) = 0.4871]
Completeness to theta = 25.000°	97.7 %
Refinement method	Full-matrix least-squares on F^2
Data / restraints / parameters	14797 / 1276 / 979
Goodness-of-fit on F^2	0.888
Final R indices [I>2sigma(I)]	R1 = 0.2413, wR2 = 0.4403
R indices (all data)	R1 = 0.6563, wR2 = 0.6663
Extinction coefficient	n/a
Largest diff. peak and hole	2.831 and -1.056 e.Å^{-3}

CCDC number: 1816731
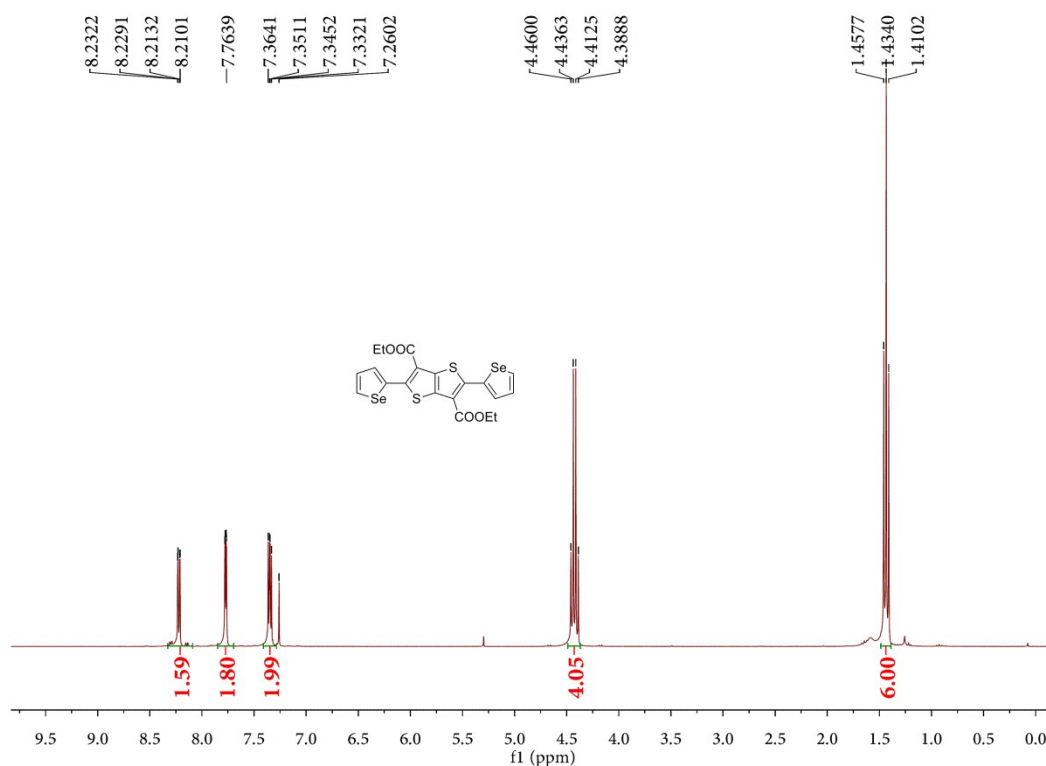
Figure S1. ^{1}H NMR spectrum of compound **3** (300 MHz, CDCl$_3$, rt).
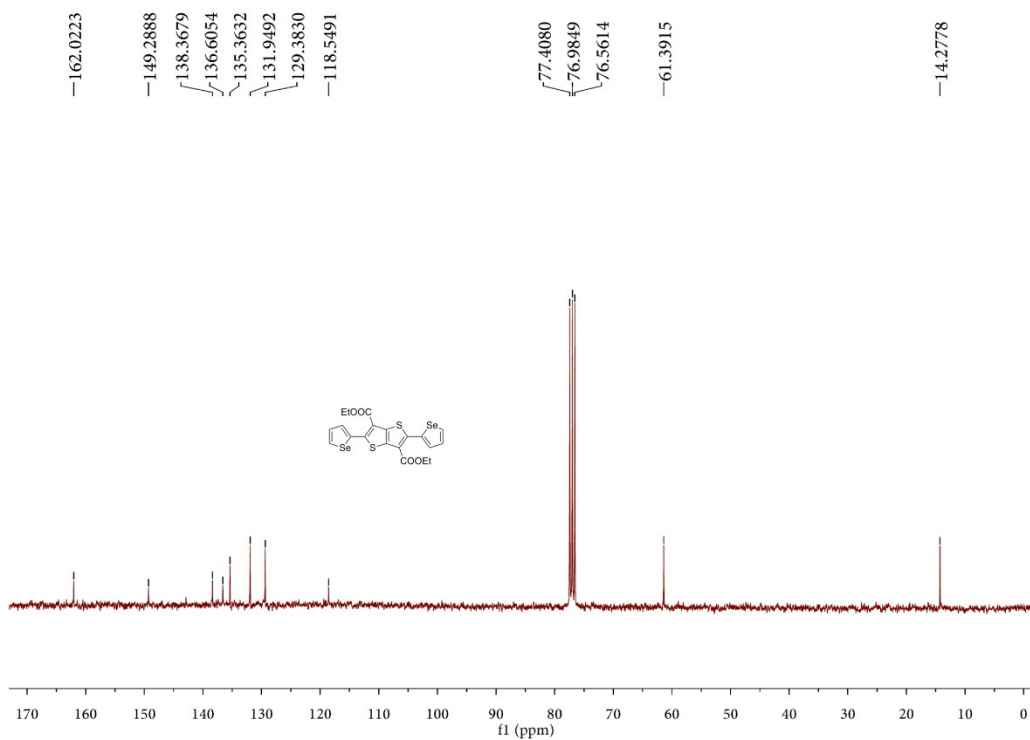
Figure S2. ¹C NMR spectrum of compound **3** (75 MHz, CDCl₃, rt).
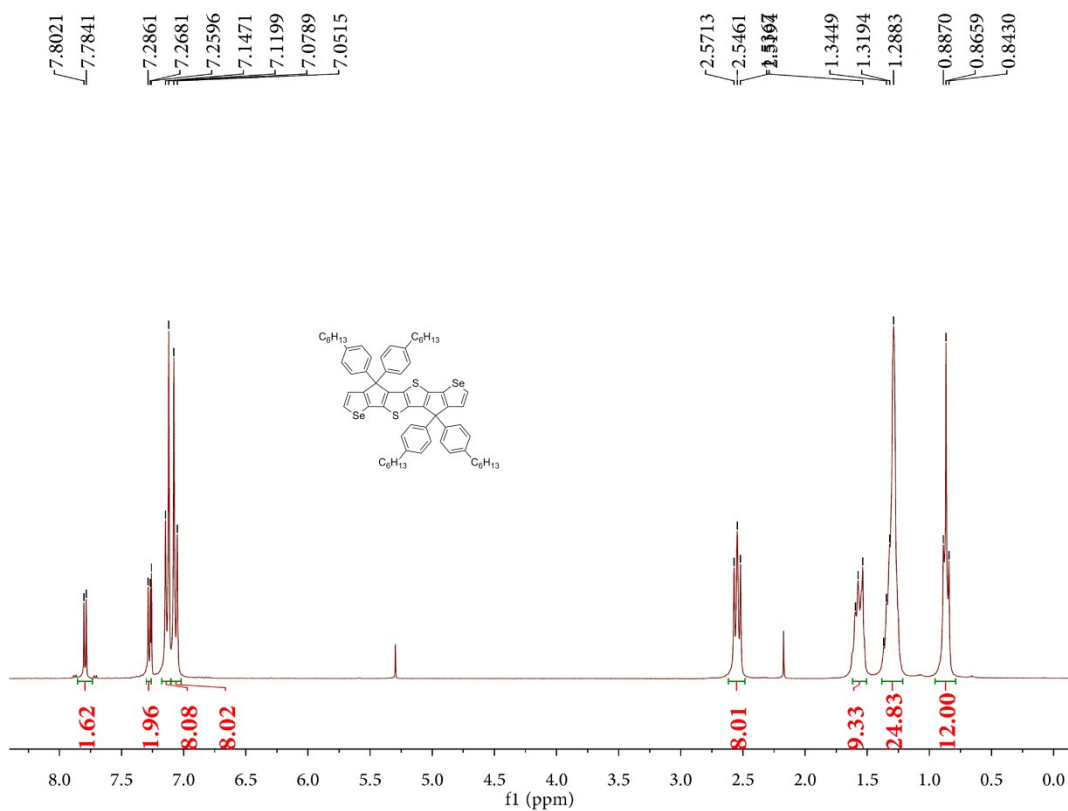
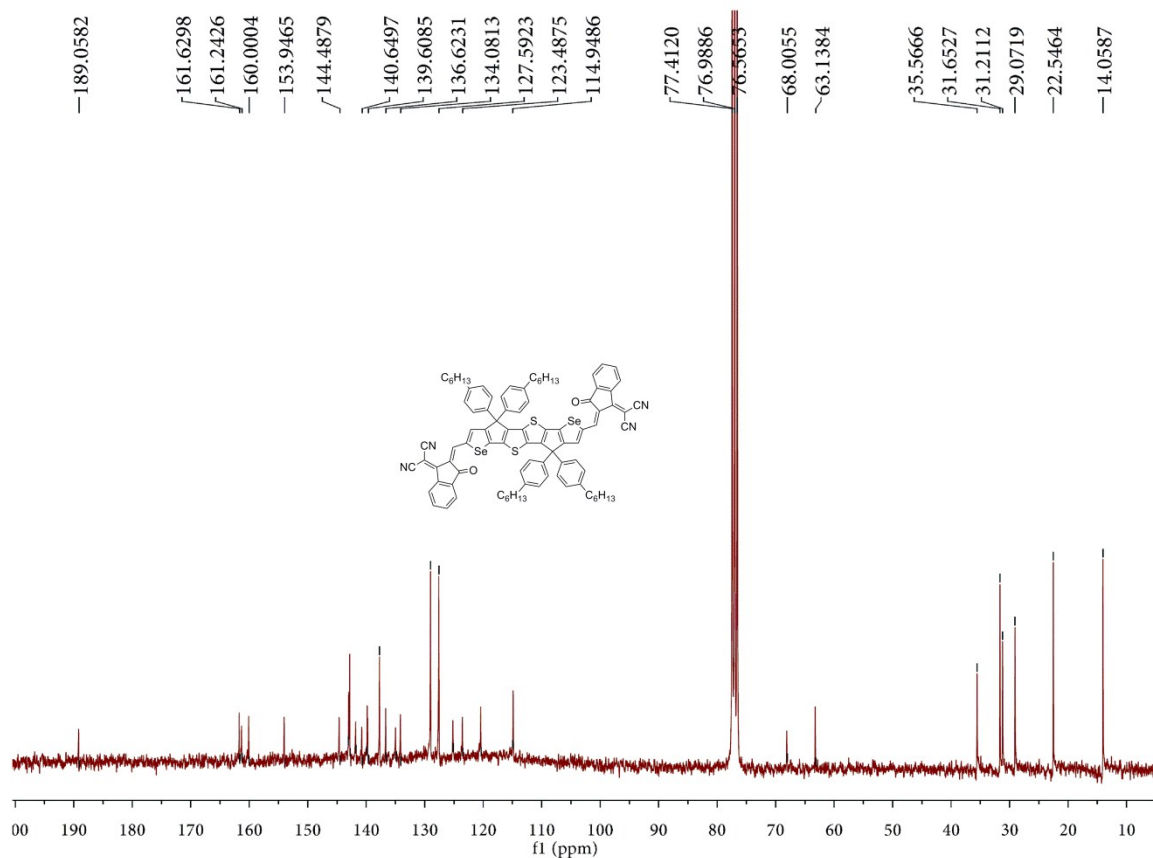**Figure S3.** ¹H NMR spectrum of compound **ST** (300 MHz, CDCl₃, rt).
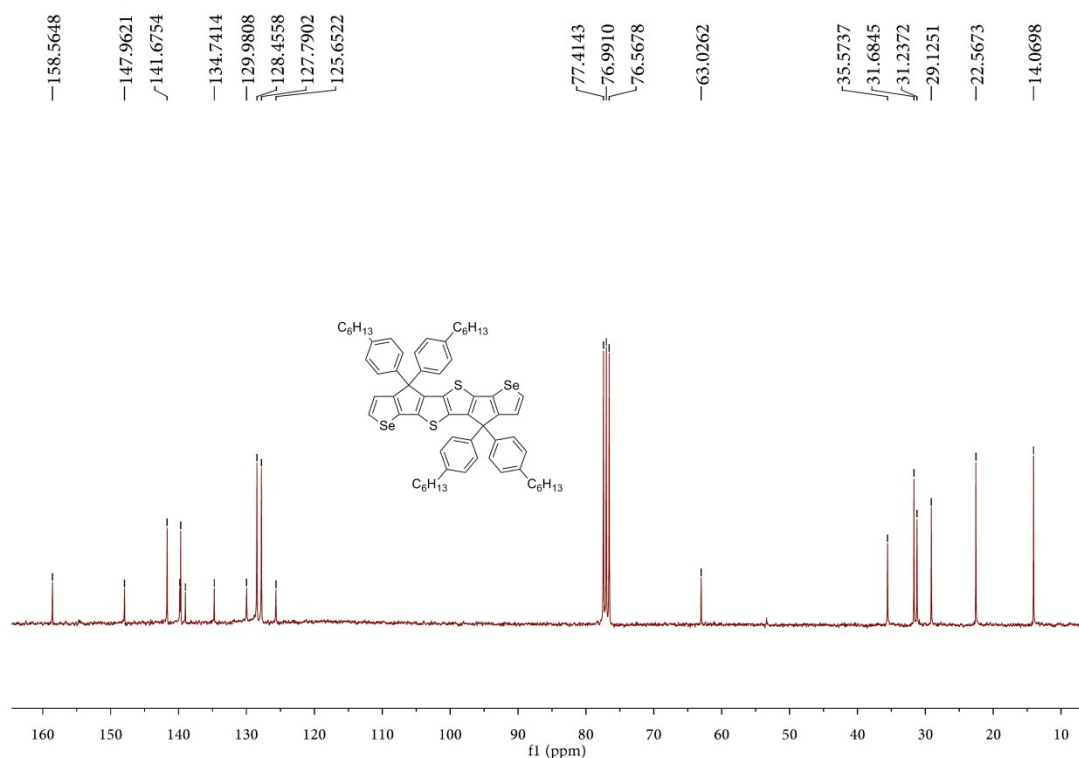
Figure S4. ^{13}C NMR spectrum of compound **ST** (75 MHz, CDCl$_3$, rt).
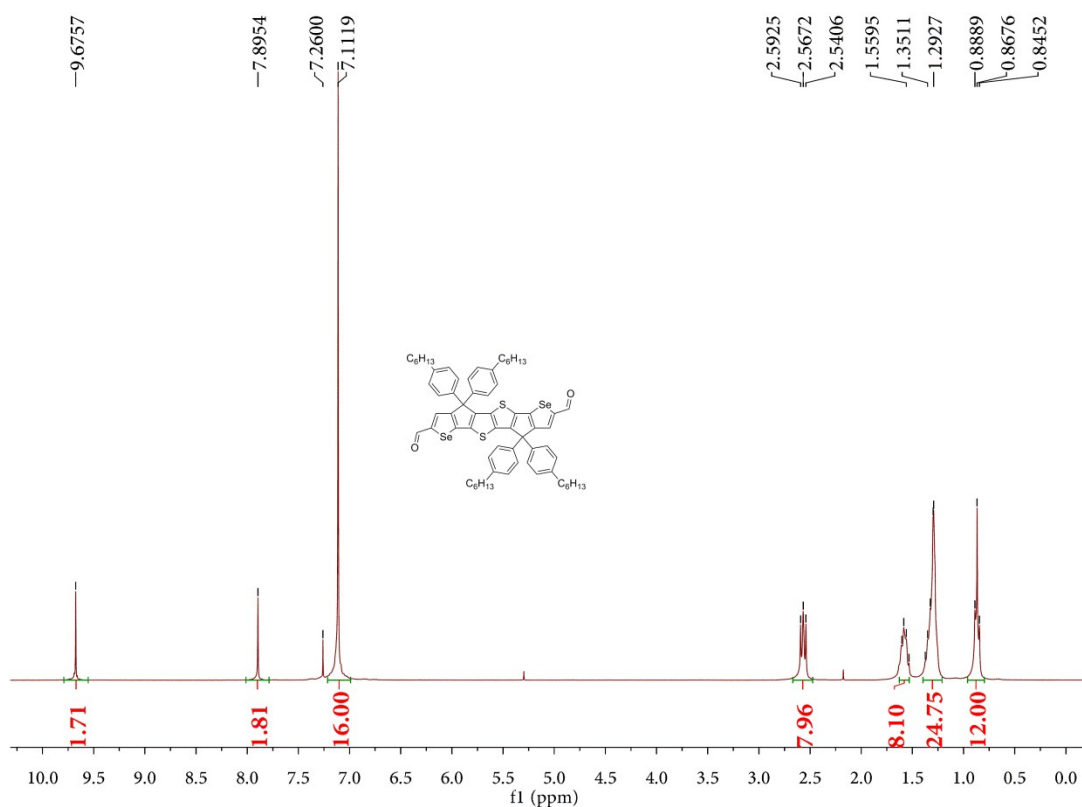
Figure S5. ^{1}H NMR spectrum of compound **ST-CHO** (300 MHz, CDCl$_3$, rt).
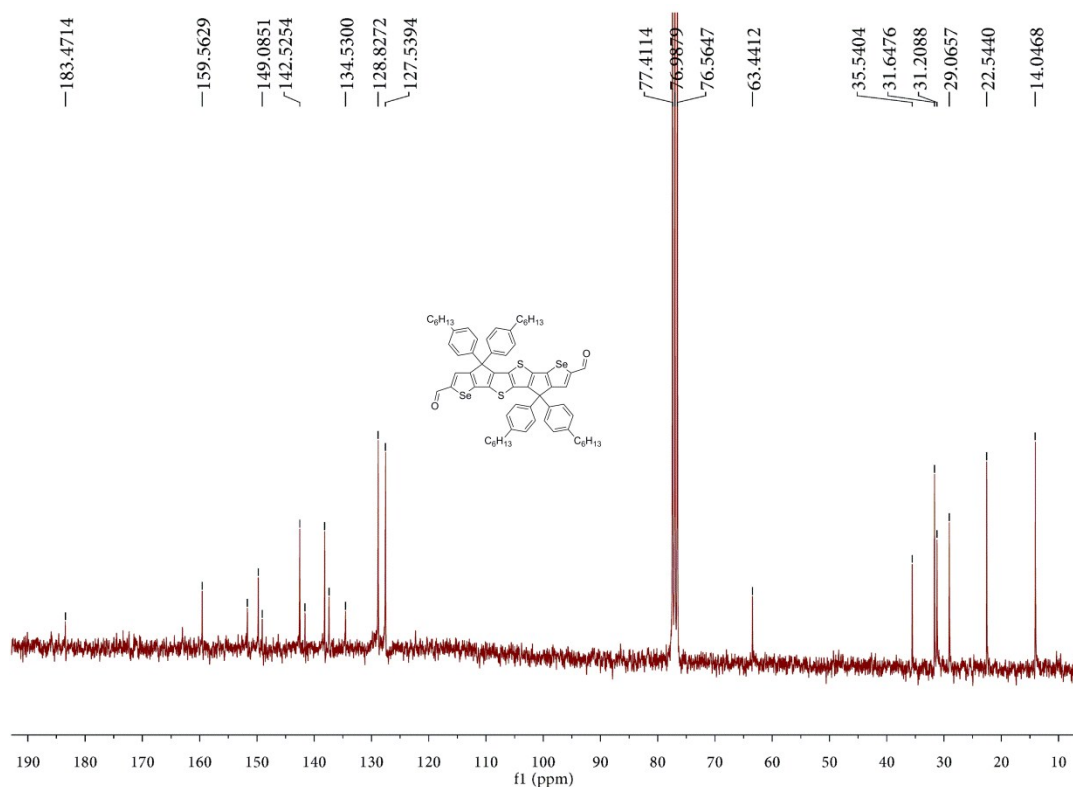
Figure S6. ^{13}C NMR spectrum of compound **ST-CHO** (75 MHz, CDCl$_3$, rt).
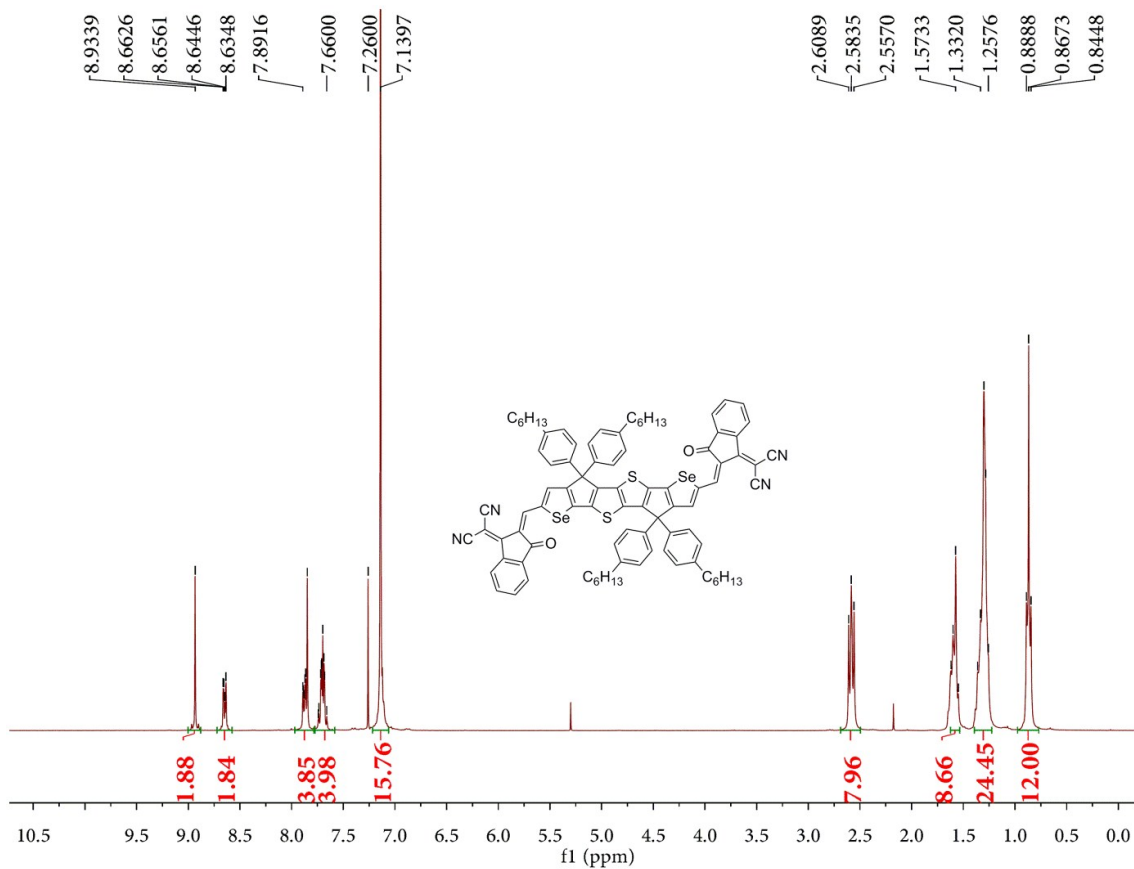
Figure S7. ^1H NMR spectrum of compound **STIC** (300 MHz, CDCl$_3$, rt).

Figure S8. ^{1}C NMR spectrum of compound **STIC** (75 MHz, CDCl$_3$, rt).
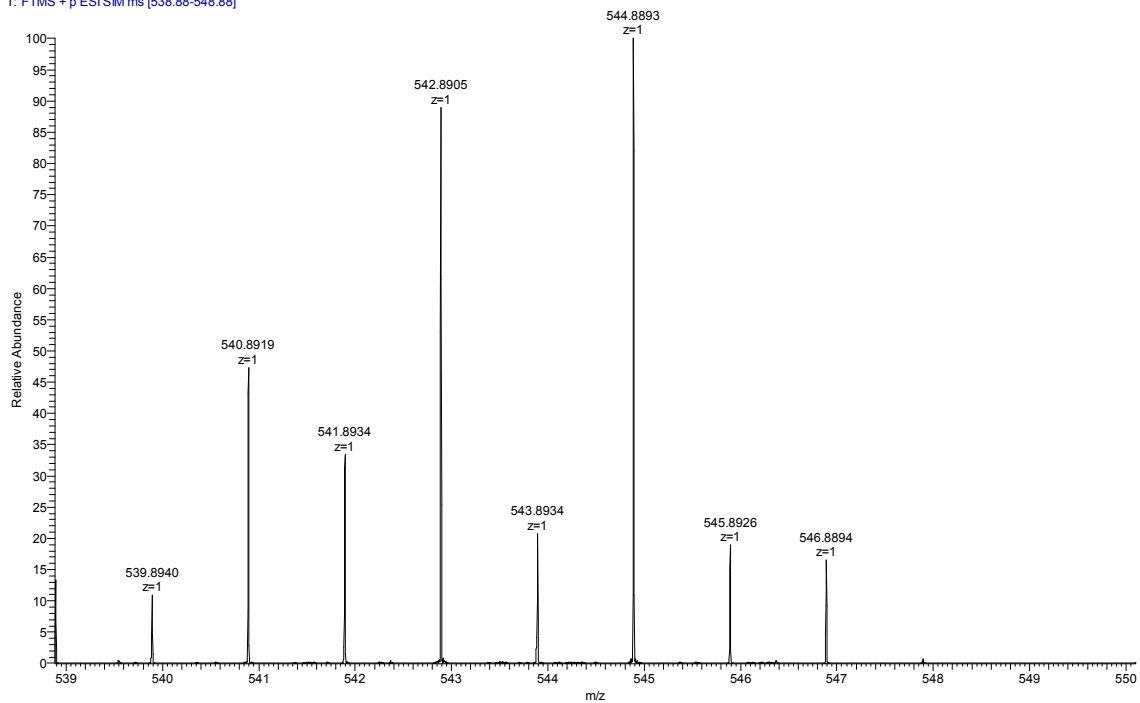
Figure S9. HRMS spectrum (ESI) of compound **3**.
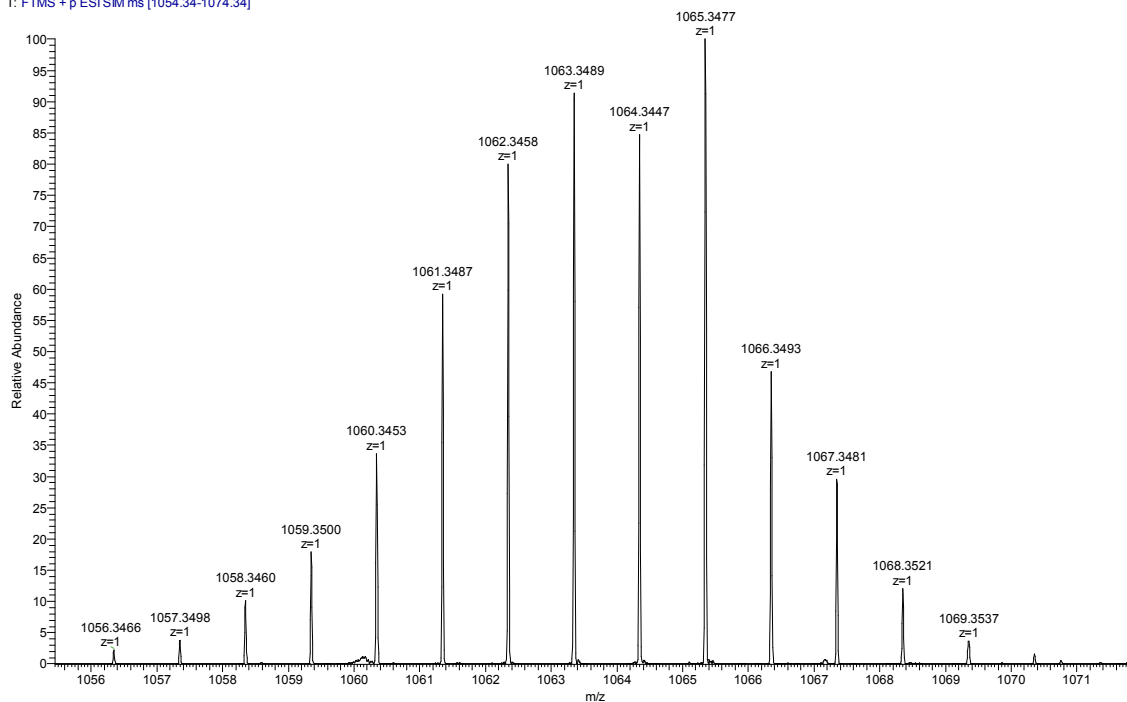
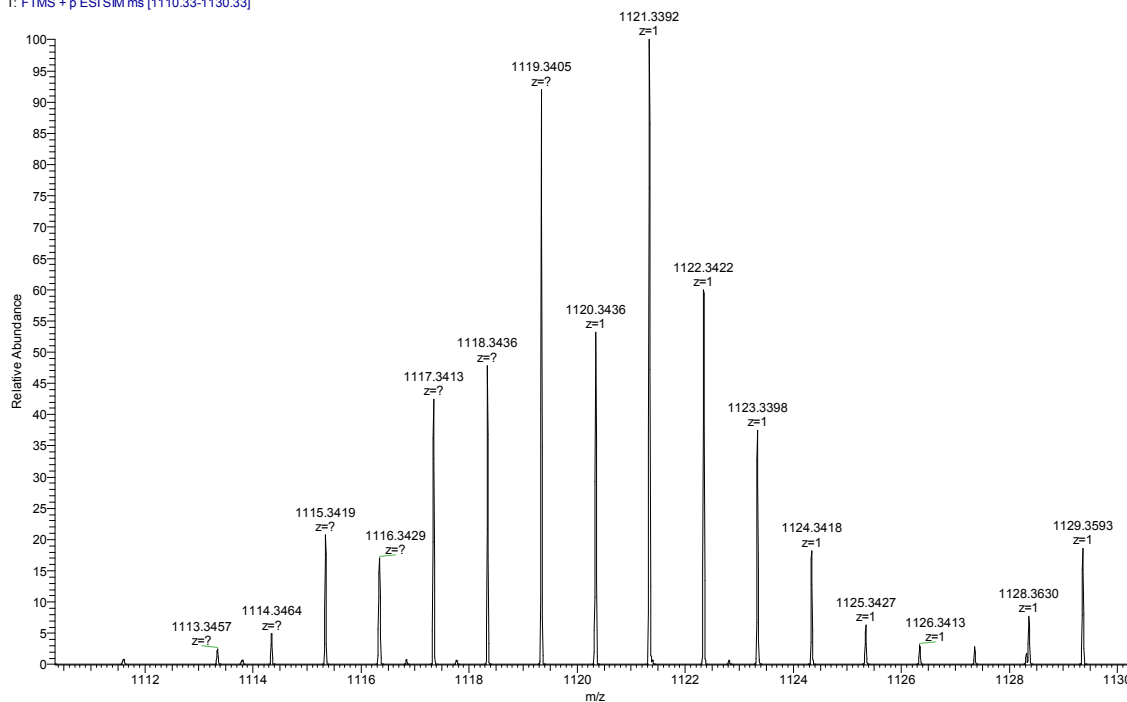**Figure S10.** HRMS spectrum (ESI) of compound **ST**.

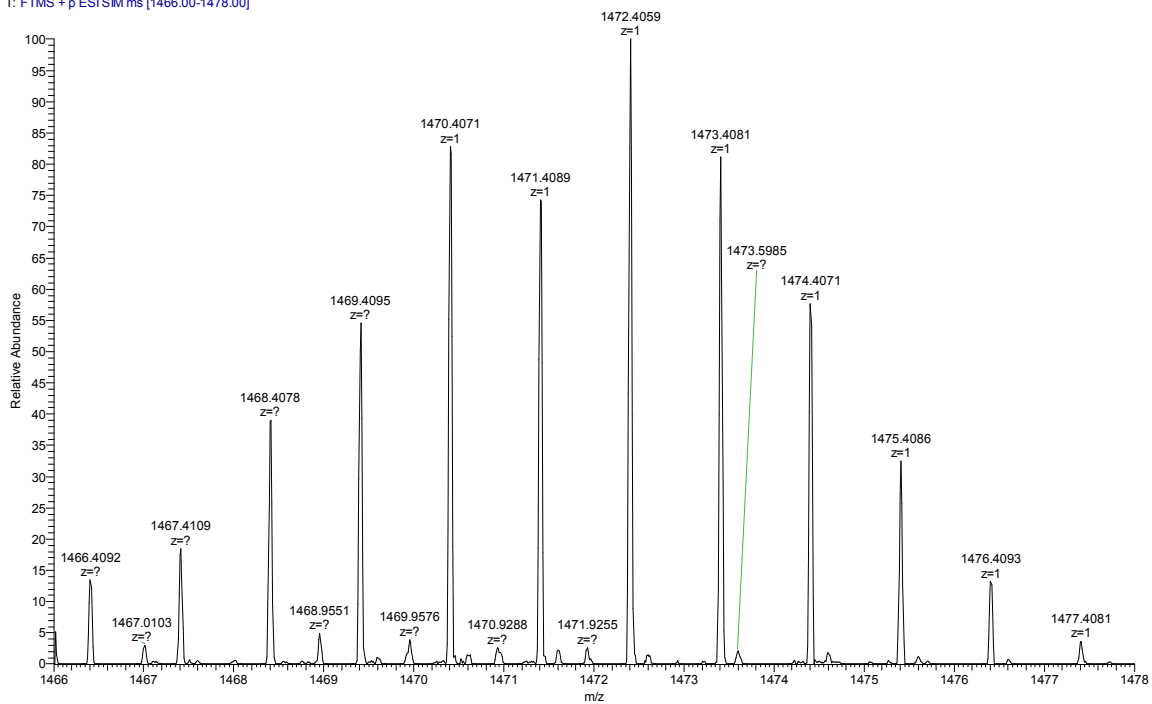**Figure S11.** HRMS spectrum (ESI) of compound **ST-CHO**.

Figure S12. HRMS spectrum (ESI) of compound **STIC**.

Table S2. Summary of the photophysical and electrochemical data.

Compound	λ_{max}^{sol} (nm)	λ_{max}^{film} (nm)	λ_{edge}^{film} (nm)	HOMO (eV)	LUMO (eV)	E_g^{EC} (eV)	E_g^{OPT} (eV)
4TIC	738	788	886	-5.28	-3.87	1.41	1.40
STIC	768	839	940	-5.20	-3.91	1.29	1.32

HOMO= - (4.8 + E_{ox}^{onset}) and LUMO= - (4.8 + E_{red}^{onset}), where E_{ox}^{onset} and E_{red}^{onset} are the onset potentials of the first oxidative and reductive waves, respectively. E_g^{EC}: electrochemical band gap. E_g^{OPT}: optical band gap estimated from the absorption onset.
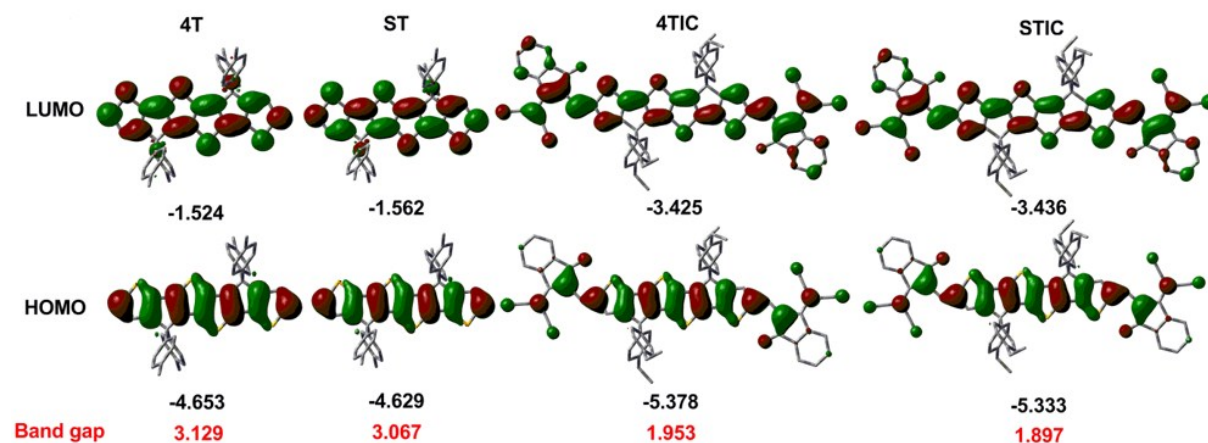
Figure S13. Simulated molecular geometries and frontier molecular orbitals obtained by density functional theory calculations for 4TIC and STIC.

Table S3. Photovoltaic parameter of OSCs based on **PBDB-T**:**NFAs**.

Compound	Treatment	V_{oc} (V)	J_{sc} (mA/cm^2)	FF	PCE (%)[a]	Calc. J_{sc} (mA/cm^2)	Voc loss (eV)
4TIC	w/o	0.819 (0.818±0.003)	17.38 (17.15±0.35)	0.62 (0.61±0.02)	8.83 (8.51±0.16)	17.03	0.581
	0.5% DIO	0.818 (0.816±0.004)	19.13 (18.89±0.38)	0.65 (0.64±0.02)	10.17 (9.8±0.18)	18.65	0.582
STIC	w/o	0.782 (0.779±0.005)	17.56 (17.42±0.28)	0.58 (0.57±0.02)	7.97 (7.65±0.24)	17.08	0.538
	0.5% DIO	0.772 (0.771±0.004)	19.96 (19.68±0.44)	0.63 (0.62±0.02)	9.71 (9.31±0.28)	19.06	0.548

[a]Average values obtained from ten devices are shown in parentheses.
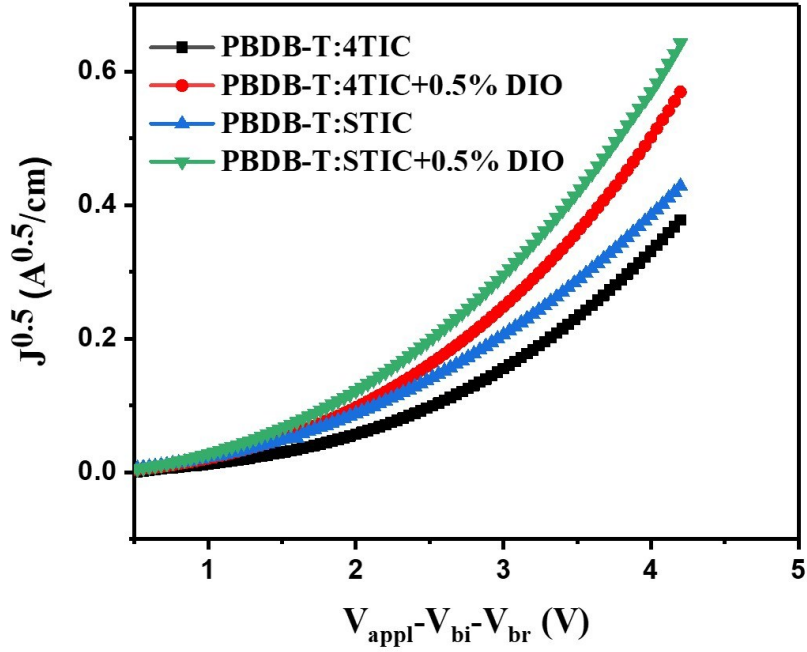
Figure S14. $J^{0.5}-V$ plots of electron-only devices with different active layers.

Table S4. Electron mobility (u_e) of different active layer based devices.

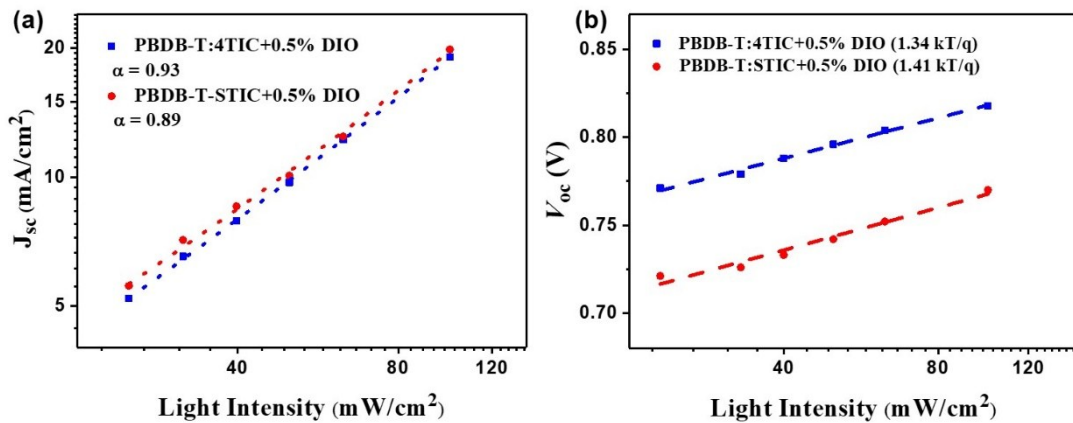| Active layer	PBDB-T: 4TIC	PBDB-T: 4TIC (0.5% DIO)	PBDB-T: STIC	PBDB-T: STIC (0.5% DIO)
u_e (10^{-5} cm^2 V^{-1} s^{-1})	4.19	9.07	5.21	12

Figure S15. Light intensity dependence of Jsc (a) and Voc (b) of the optimized device.
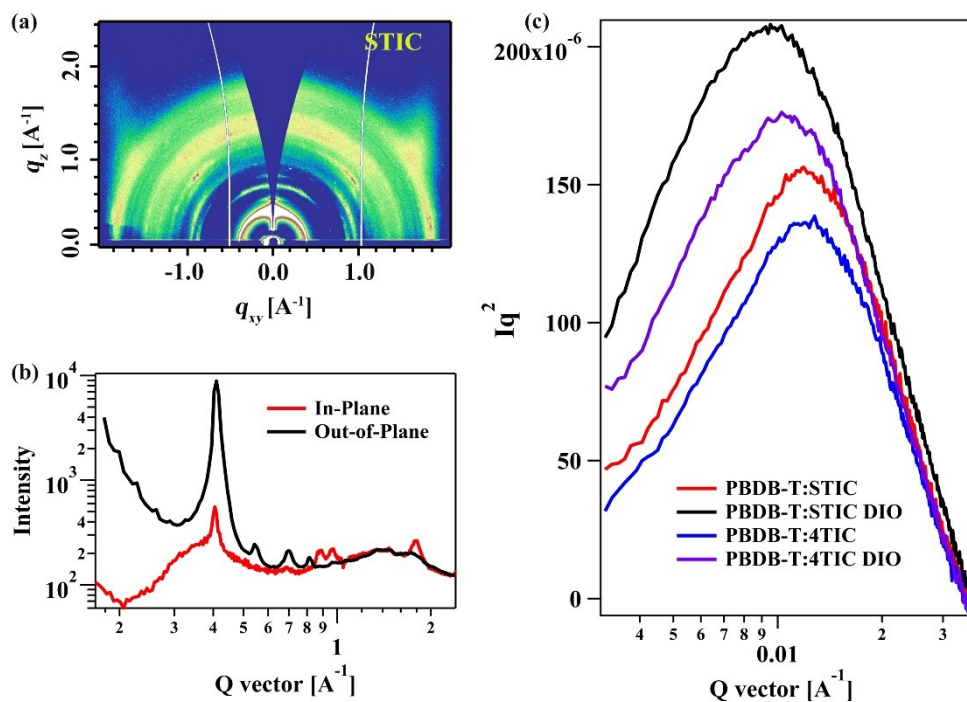
Figure S16. (a) 2D GIXD profile of STIC pure film. (b) Out-of-plane (red line) and in-plane (black line) line cut of GIXD results. (c) RsoXS profiles (Iq^2 versus q) of BHJ blends.

Table S5. Fitting results of 1D GIXD results.

Condition	Q (Å^{-1})	FWHM (Å^{-1})	Peak Area	D-spacing (Å)	Crystal Coherence Length (Å)
PBDBT:STIC	1.71	0.350	245.97	3.67	16.16
PBDBT:STIC DIO	1.75	0.297	289.22	3.59	19.04
PBDBT:4TIC	1.71	0.372	177.34	3.67	15.20
PBDBT:4TIC DIO	1.73	0.310	199.51	3.63	18.24